# QUALITY CONTROL AND FILTERING OF SATELLITE DATA

P. Lönnberg
European Centre for Medium Range Weather Forecasts
Shinfield Park, Reading

## 1. INTRODUCTION

The most extensive observational coverage of the atmosphere is provided by space based observing systems. However, the satellites observe quantities which require transformations to the variables of the atmospheric models. These transformations introduce significant systematic and random errors which complicate the quality control (QC) and the use of these data in an analysis scheme. Special QC algorithms must be constructed to detect problems with satellite data. The importance of efficient QC has increased rapidly because with increased analysis resolution the forecasts have become very sensitive to (bad) satellite data (Andersson et al., 1989 and Lönnberg, 1988). The QC procedures for satellite data in the ECMWF analysis are described in Section 2. More sophisticated QC algorithms which are planned for implementation in future versions of the ECMWF analysis are presented by Kelly et al. (1989).

The use of (quality controlled) satellite observations, in particular thicknesses, requires special attention due to the complicated error structures in these data. Furthermore, the vertical resolution of the satellite information is less than the resolution of the forecast model. This means that only the deep structures can be seen by the satellites and the finer details in the vertical are imposed by the specified prediction error covariances. A noisy temperature profile on model levels may easily result from improper tuning of the observation and forecast error statistics of the analysis scheme. The filtering of observation noise and the interpolation from the data to model levels are discussed in Section 3. Some concluding remarks are made in Section 4.

## 2. QUALITY CONTROL

The ECMWF analysis QC is sequential with tests of increasing severity. Basically, a datum which fails a test is not considered any further. The checks are made against independent estimates of what the observed value ought to be. In data rich regions the test against an independent analysis using neighbouring observations is usually very efficient in detecting erroneous observations or extreme atmospheric events which are beyond the resolution of the analysis scheme. However, the main problems occur in data sparse regions which are mainly observed by satellite data.

2.1 Check against the first-guess

The background field is usually the only reliable independent source of information against which observations can be checked over oceans. In the ECMWF analysis the test is simply a comparison of the observed departure from the background field against the estimated distribution of this quantity. Departures exceeding a certain tolerance, i.e. p standard deviations, are regarded as observation errors and are hence rejected. The probability of gross errors for a particular observing system influences the setting of rejection limits. The test is scalar for heights and thicknesses, while for winds the test is performed on the vector difference between observed wind and background wind.

(i) Winds

A wind observation $W_{ob}$ is rejected if the following statement is true:

$$(W_{ob} - W_{fg})^2 > p^2 (E_{ob}^2 + E_{fg}^2)$$

where subscripts ob and fg refer to observation and background

E is the standard deviation of the error

p is the rejection limit

We can estimate the observation and forecast error variances quite accurately from past performance of the observing systems and the data assimilation schemes. The critical tuning parameter is p. For standard pressure level radiosonde winds, which in the ECMWF analysis scheme are regarded as the most reliable winds, p is set to 4.5.

Winds derived from the movement of clouds may not necessarily be representative of the air flow (Schmetz, et al. 1989 and Radford, 1989). In particular, upper level cloud motion winds (CMWs) near jet streams tend to underestimate the strength of the jet (Fig.1). The dashed line in Fig. 1 is the linear regression between the observed wind speed and the first-guess wind speed. The bias towards low observed winds in jet streams is quite obvious from Fig. 1. For other wind observing systems no such biases have been found. As the bias at strong winds usually occurs in baroclinic regions the use of such winds might be very detrimental to the forecasts (Kelly and Pailleux, 1989). Because of these problems, an asymmetric test of CMWs has been implemented. Two values for p are used: 0.95 and 1.3. The smaller value is used in the extratropics (polewards of 30 degrees latitude) for upper level winds (pressure less then 500 hPa), when the first-guess wind speed exceeds 30 m/s and the observed wind speed is more than 7.5 m/s weaker than the guess. The larger value is used in all other circumstances. The effect of these rejection limits can be seen in Fig. 2 in which the departures from the first-guess (magnitude of

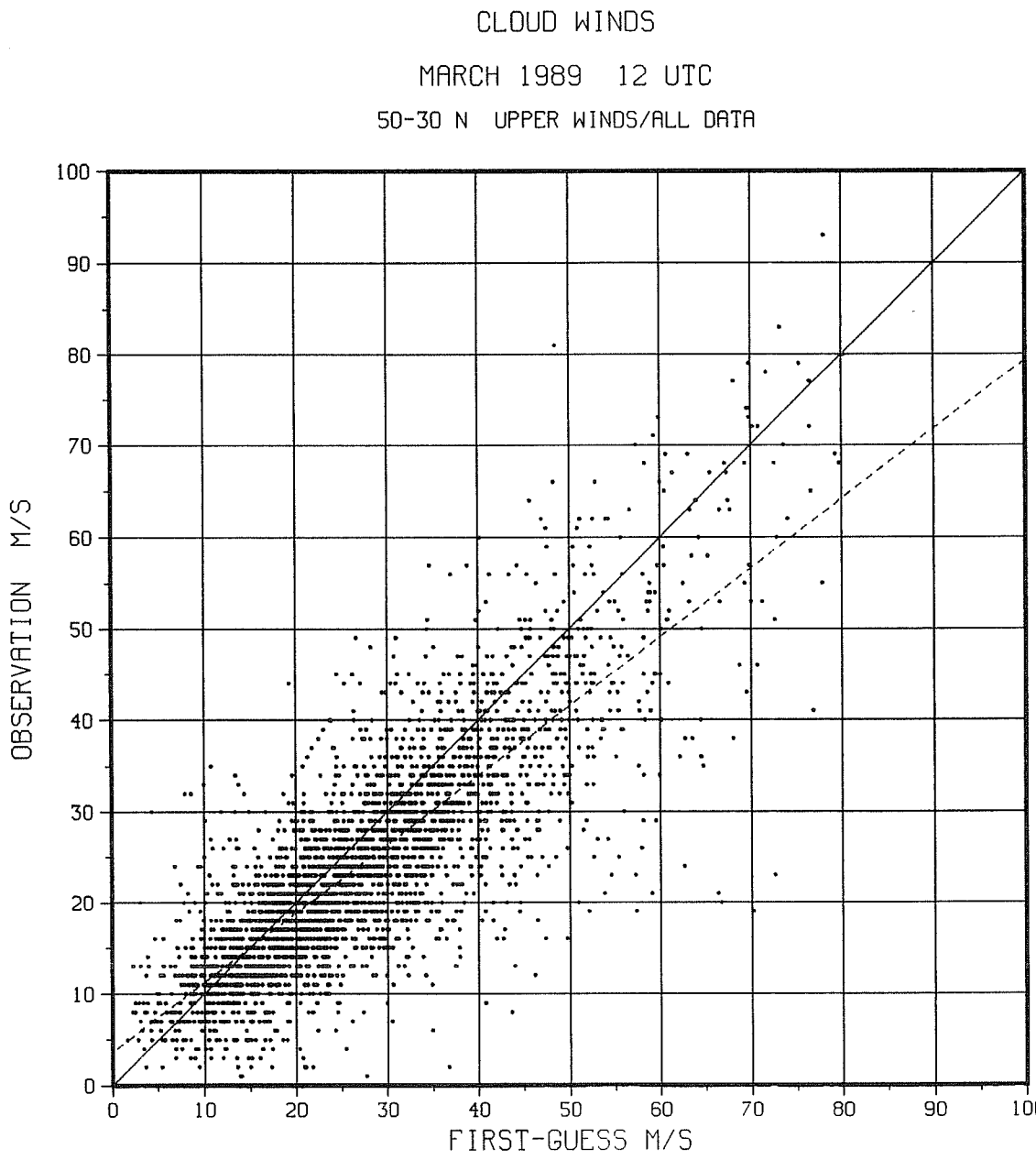


Fig. 1 Scatterdiagram of observed cloud motion wind speed against first-guess wind speed for all upper level winds in March 1989 12 UTC between 30 and 50 N. The dashed line is a linear regression of the observed wind against the first-guess wind speed.

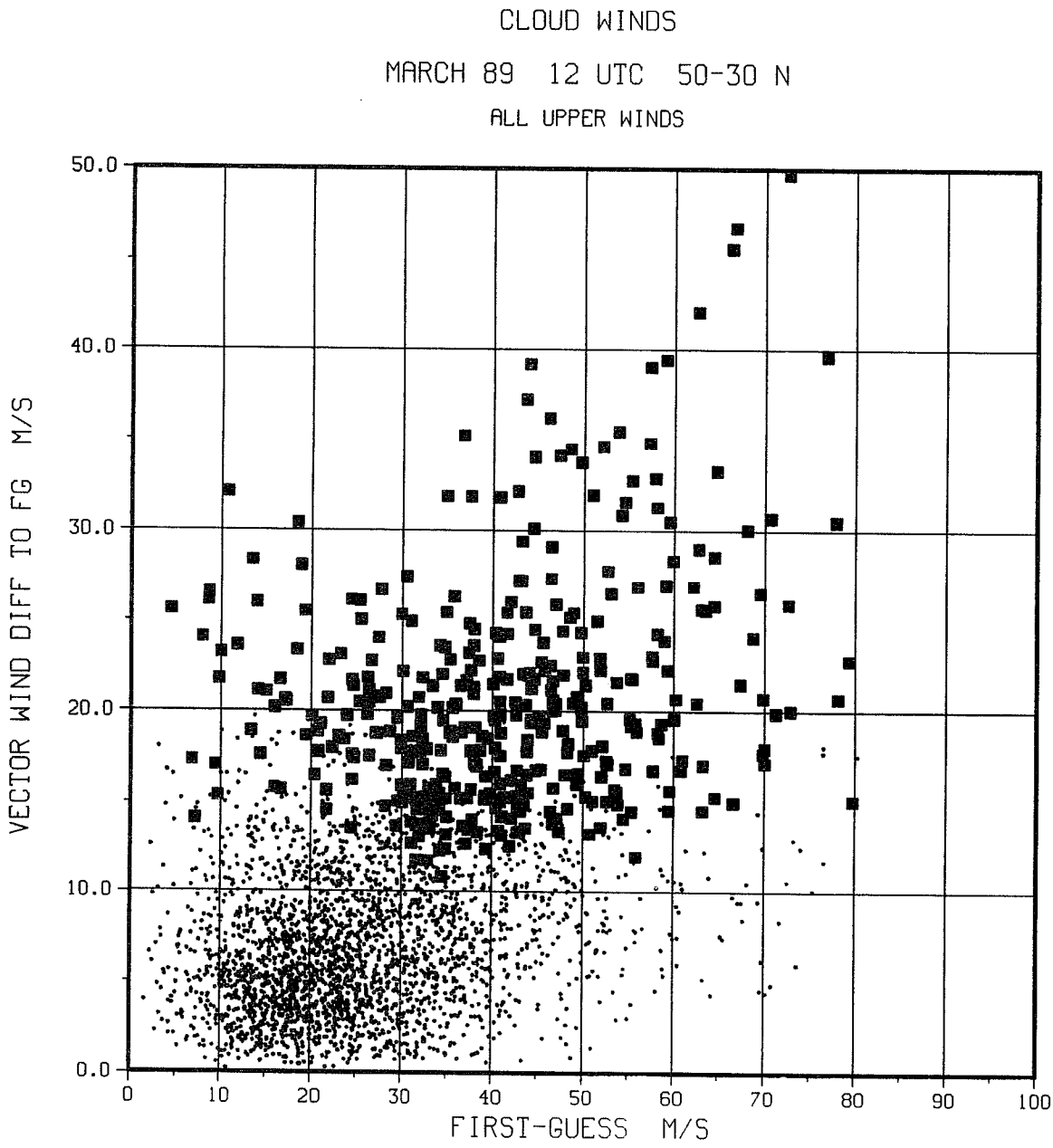


Fig. 2 Scatterdiagram of magnitude of vector wind difference observed and first-guess wind as function of first-guess wind speed. The data set is the same as in Fig. 1. The small dots are used winds and the large squares are rejected cloud motion winds.

vector wind difference) are stratified according to the background wind speed. The used data are indicated by small dots, while the rejected winds are indicated by squares. The asymmetric nature of the CMW rejections, i.e. higher tolerance for weaker than stronger winds is quite clear from Fig. 2. A disturbing feature of Fig. 2 is the existence of very large deviations from the background. The CMW rejection limits have been tuned based on synoptic evaluation and forecast experiments.

(ii) Thicknesses

Multi-level data pose a different kind of QC problem. Their impact on the analysis and forecast is much stronger, but there are more ways of identifying erroneous profiles. The satellite thicknesses are a rather special type of observations which require complicated QC algorithms to identify erroneous satellite soundings. There are three steps in the QC of satellite thicknesses against the background:

(a) Test every individual layer for excessive departure
(b) Combine the results of (i) for all layers in one profile
(c) Test the gross tropospheric stability

Each thickness departure is compared to the combined distribution of the observation and forecast errors. QC flags ranging from 0 to 3 are set for each datum. Any datum with a flag 3 is rejected. The flag 3 limits as a function of pressure are:

| hPa | 1000 - 700 | 700 - 500 | 500 - 300 | 300 - 100 | 100 - 50 | 50 - 30 | 30 - 10 |
|---|---|---|---|---|---|---|---|
| STD | 1.2 | 2.1 | 2.75 | 2.75 | 2.75 | 2.6 | 2.3 |

The tighter rejection limits in the lower troposphere and for the layer 10/30 hPa reflect the poor quality of the data for those layers. The limits for flag 1 and 2 are lower and proportional to the flag 3 values.

The whole flag pattern for a satellite sounding is utilized in the multi-layer test. According to the distribution of the flags the whole sounding might be rejected.

A third test is applied to satellite thicknesses. The gross tropospheric stability of a satellite sounding is compared to the first-guess stability (Andersson, pers.comm.) and a sounding is rejected if it fails the test:

$$|T'(1000\text{-}700) - T'(500\text{-}300)| > 3.5 \text{ K}$$

where $T' = T_{ob} - T_{fg}$

If as a result of the QC the remaining satellite sounding is incomplete, the whole sounding is rejected. This means that over oceans, complete profiles between 1000 and 10 hPa are used, while over land 100 to 10 hPa profiles are used. An example of the efficiency of the stability check is shown in Fig. 3. The scatter of the observed stability compared to the forecasted one is very large. Similar statistics for Ocean Weather Ships in the Atlantic have much smaller scatter (not shown). The filled circles are the used data, while open circles are the rejected ones. Most of the satellite sounding rejections are caused by incorrect observed static stability.

2.2 Check against independent analysis by statistical interpolation

The statistical interpolation or OI check is similar to the first-guess check. The departure of the observation from an independent analysis using neighbouring data is compared to the expected distribution of this quantity:

$$(O - A)^2 > s^2 (E_o^2 + E_a^2)$$

where O and A are the observed and analysed values respectively and

$E_o$ is the observation error estimate

$E_a$ is the analysis error estimate, which consists of the OI analysis error estimate and an estimate of the analysis error of the unresolved scales.

The values for s are 3 standard deviations for wind and 1.2 for thicknesses again reflecting the high uncertainty of satellite soundings. In checking CMWs or satellite thicknesses, the independent analysis is formed without data of the same type, e.g. a CMW datum is checked against an analysis without any CMWs. The analysis increments are calculated separately for the troposphere and the stratosphere with some overlap in data selection and the levels at which the increments are calculated. If there is a gap in the selected part of a satellite sounding then the sounding is not used for analysis of that part of the atmosphere.

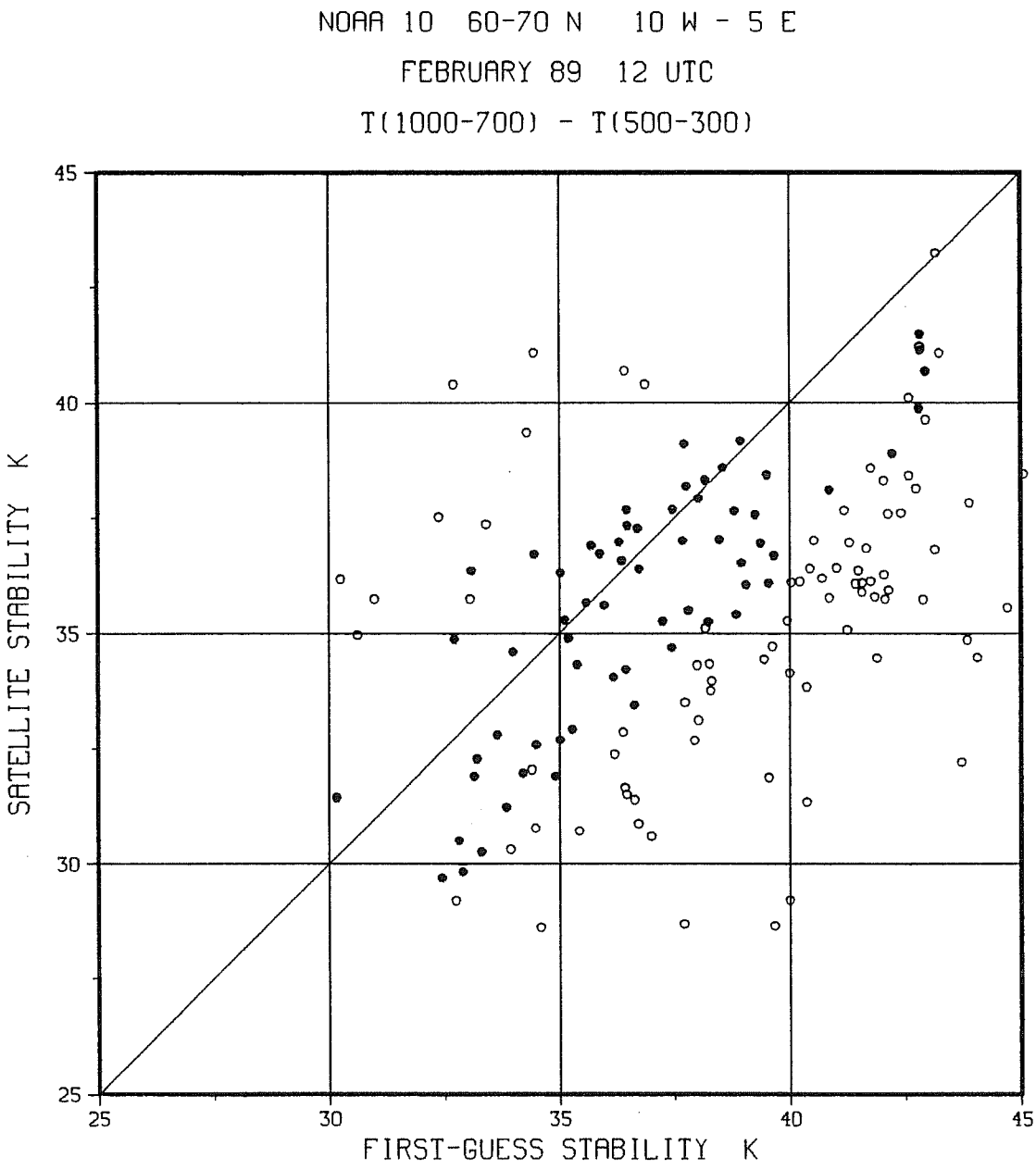


Fig. 3 Scatterdiagram of observed temperature differences between layers 1000-700 hPa and 500-300 hPa compared to the first-guess temperature differences. The data is all NOAA10 soundings in February 89 at 12 UTC between 60 and 70 N and 10 W and 5 E. The filled circles are used data and open circles are rejected observations.

## 2.3 The tail of the distribution of first-guess error

Quality control of observations in data sparse regions is one the most difficult problems in data assimilation. The only available independent estimate is usually the background field, i.e. the six hour forecast. It then becomes essential to determine the error of the background as accurately as possible. Since we lack dynamic estimates of the forecast errors as given for example by a Kalman filter, it is necessary to estimate the error from reliable data, ideally for every analysis time. The statistical distribution of the forecast error provides good guidance in setting limits for rejecting data. Stations and observing systems which have been found to produce reliable data can then provide a map of suitable rejection limits.

We have investigated the tail of the distribution of the magnitude of the vector wind difference between observation and background for two observing systems, radiosondes and CMWs. Fig. 4 shows the North American radiosonde stations. In this figure 10% of the departures observation-minus-background exceed the value shown. The lowest numbers are 11 m/s for stations with low random wind error and for which the probability of gross errors is less than 10%. A few stations have clearly higher values than their nearest neighbours, pointing to some problems at those stations. The corresponding values at the 2% level are shown in Fig. 5. Values as low as 15 m/s are found in continental North America. Many of the west coast stations, which are exposed to advection of a poor 6 hour forecast, have values well below 20 m/s at the 2% level.

Similar plots of the geographical distribution have been produced for CMWs in boxes of 5 degrees latitude and 10 degrees longitude. At the 10% level (Fig. 6) the geographical distribution of the values is rather homogeneous. The numbers are clearly higher than the radiosonde ones, even in boxes near the coast. The highest values out in the Pacific are much higher than any radiosonde value at the 10% level. This is partly due to somewhat higher first-guess errors, although the Aleutian sonde stations suggest that the oceanic forecast errors (Fig. 4) are only slightly higher than the continental errors. The problems with CMWs are evident already at the 10% level. The CMW departure values at the 2% (Fig. 7) level are significantly higher than those for the radiosondes. Some boxes show very large values which suggests that the likelihood of gross errors is substantial for CMWs.

From the extreme parts of the distributions it is possible to estimate the relative usefulness of different observing systems and the probability of gross errors. The distribution of departures at reliable stations could serve as guidance in setting the rejection limits.

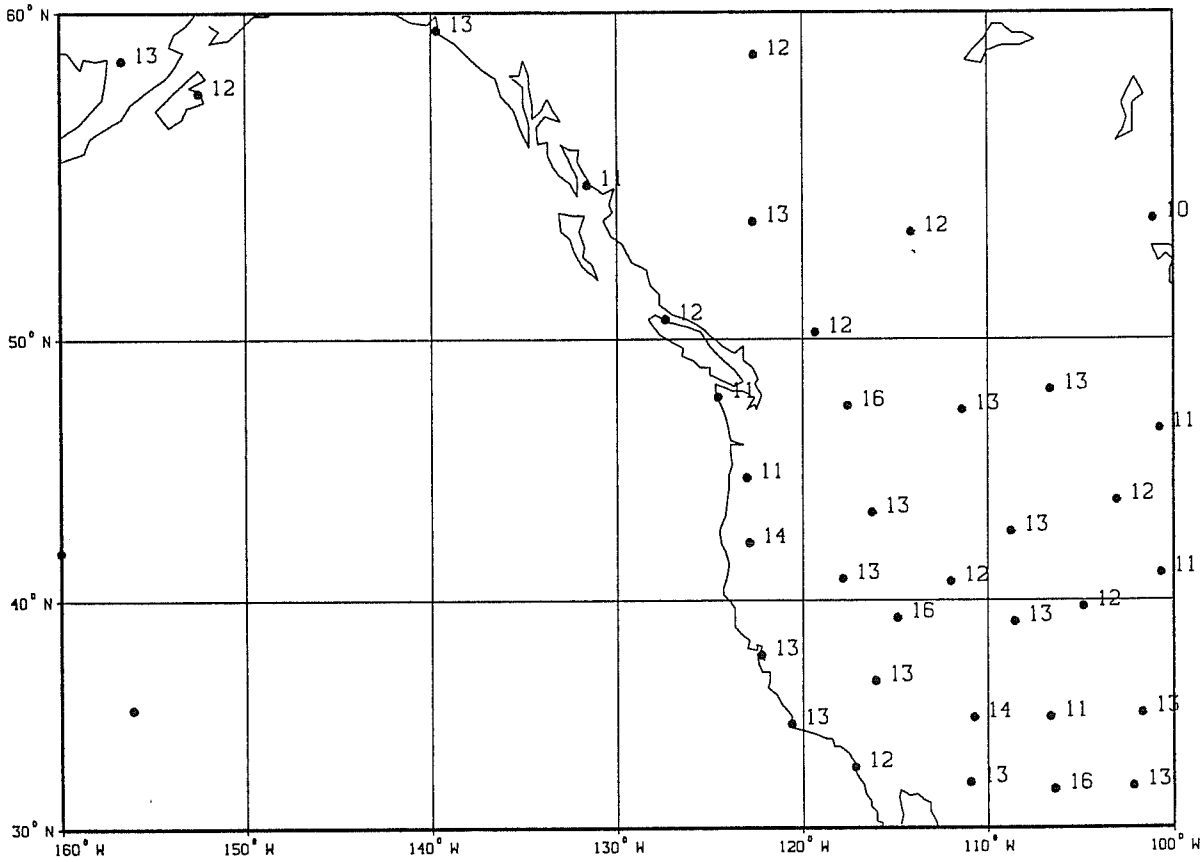


Fig. 4 Magnitude of vector wind difference between 300 hPa radiosonde observation and background at 10% level, i.e. 10% of the departures at a station exceed the value shown. The data set is all radiosonde winds in December 88 - February 89 at 0 and 12 UTC.

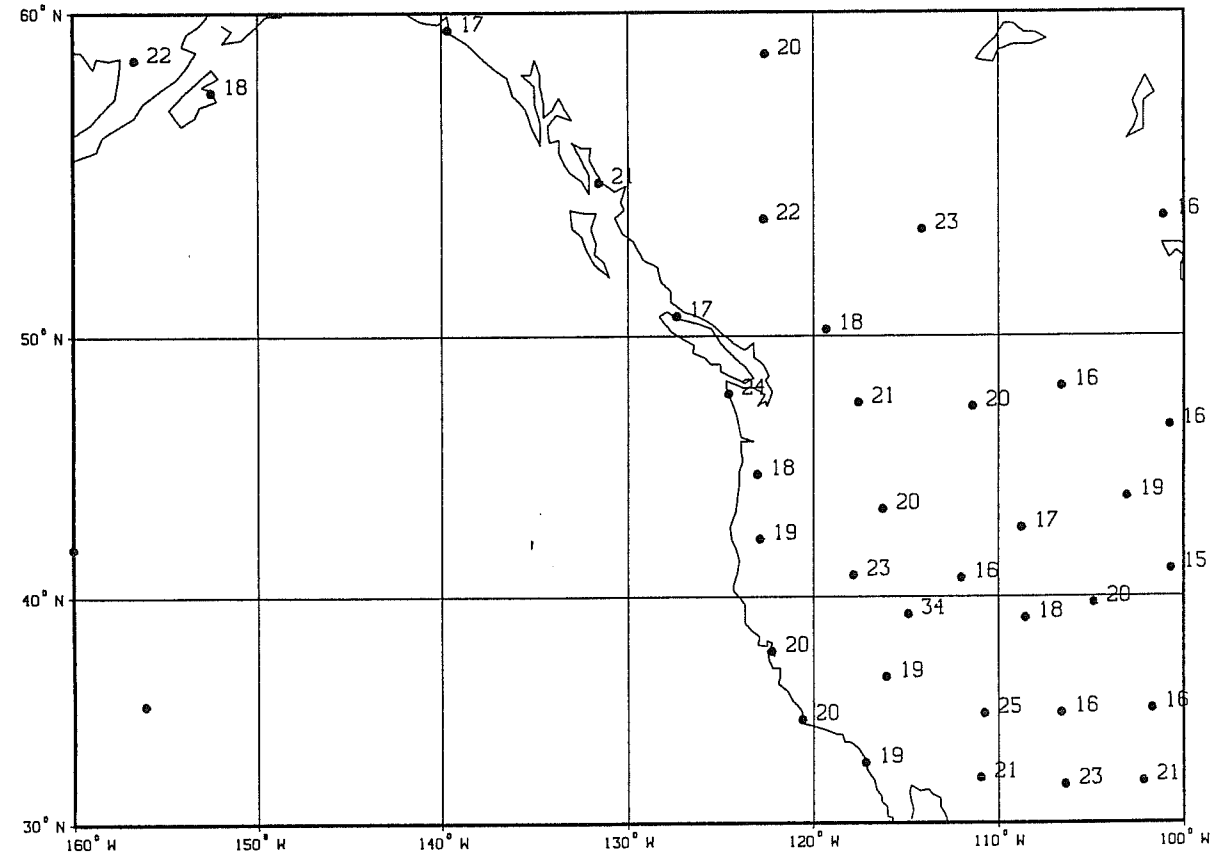


Fig. 5 Same as Fig. 4, but at 2% level.

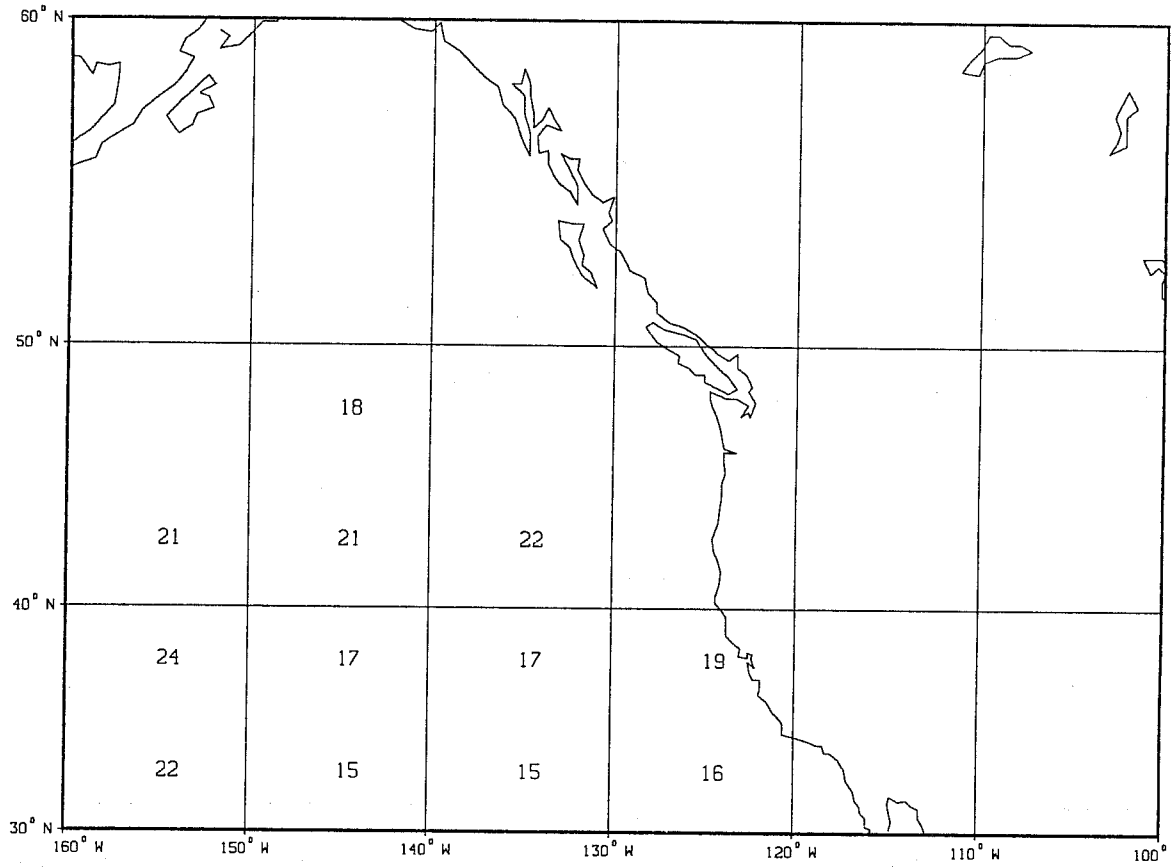


Fig. 6 Same as Fig. 4, but for cloud motion winds. The winds have been collected in box of 5° latitude and 10° longitude approximately centred at the numbers shown.

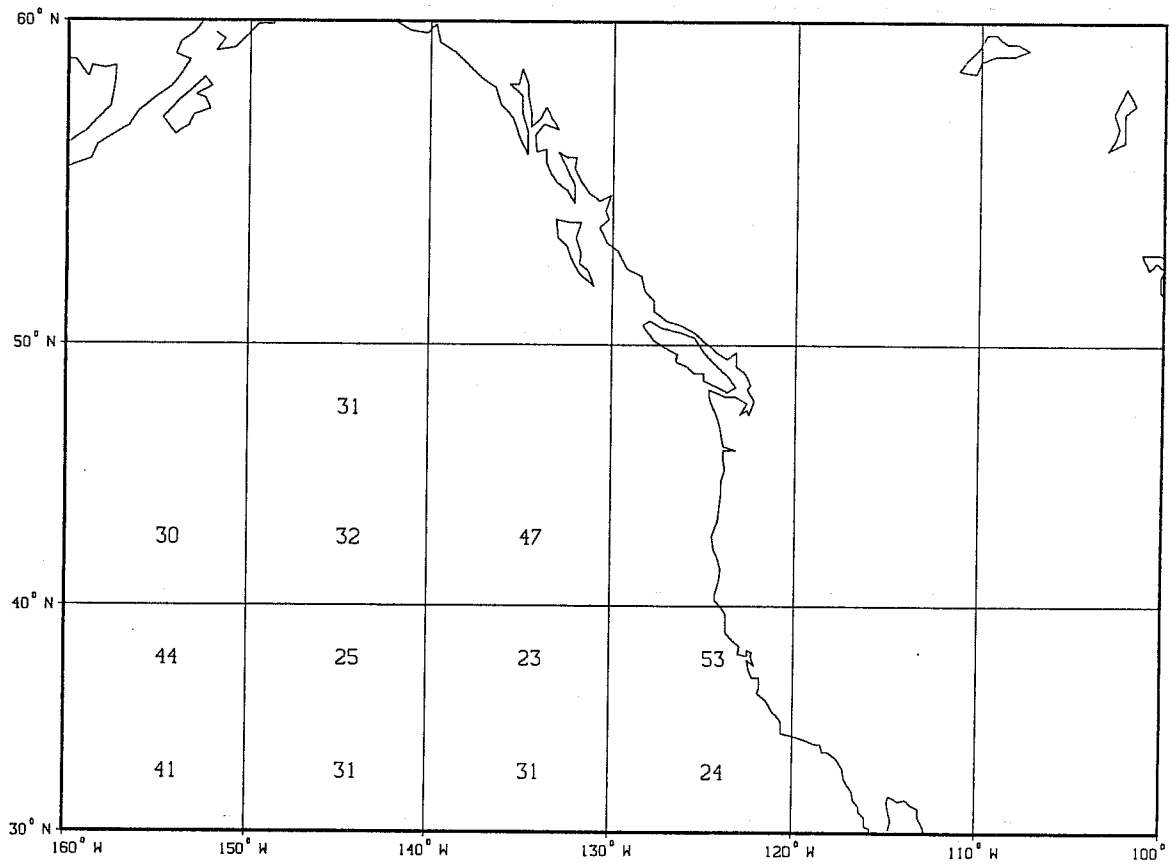


Fig. 7 Same as Fig. 6, but at 2% level.

## 3. FILTERING OF SATELLITE DATA BY OI

The complicated error structures of the satellite thickness data make proper tuning of the OI statistics necessary. OI requires knowledge of the error structures of the observations used. This a serious concern with satellite thickness data. If error covariances are derived from unscreened data like those shown in Fig. 3. the result is different to that obtained by quality controlling the data strongly first and then calculating the error covariances (Strauss,1989). The structure of the observation error covariances together with the forecast error covariances determine the response of the OI algorithm. The satellite thickness observation error covariances used at present in the ECMWF analysis are based on data sets with screening of very rough errors only (Kelly and Pailleux, 1988). The resulting error correlations have only small off-diagonal elements. The small values of these are probably caused by the excessive noise in the data. Use of such observation error covariances leads to a rather undesirable response by the OI algorithm. Two aspects of the OI response to satellite thicknesses will be discussed in the following: filtering of the data and interpolation of the filtered data to model levels.

### 3.1 Filtering of satellite data

A very powerful tool to investigate the response of the OI system to observations is decomposition of the weight matrix into its eigenvalues and vectors (Hollingsworth and Lönnberg, 1986). In particular, the analysis at the observation points will be studied. The weight matrix $\underline{\underline{W}}$ for the analysis at the observation points has the following form:

$$\underline{\underline{W}} = \underline{\underline{P}} \, (\underline{\underline{P}} + \underline{\underline{O}})^{-1}$$

where $\underline{\underline{P}}$, and $\underline{\underline{O}}$ are the prediction and observation error covariance matrices between observation points.

In the following, we will study the properties of $\underline{\underline{P}}$, $\underline{\underline{O}}$ and $\underline{\underline{W}}$ as set up in the ECMWF analysis scheme, i.e. separate tropospheric and stratospheric analyses. We will only look at the tropospheric response as most of the problems with satellite data occur in the troposphere. For the tropospheric analysis, 4 thicknesses are selected from one satellite profile. The eigenvalue and vector decomposition is then done for a single profile with 4 data items, leading to a 4 by 4 matrix problem. Fig. 8 shows the eigenvalues and vectors of the P matrix where the elements of the matrix represent the prediction errors of the thicknesses for the layers 100-300-500-700-1000 hPa. The mode with the smallest

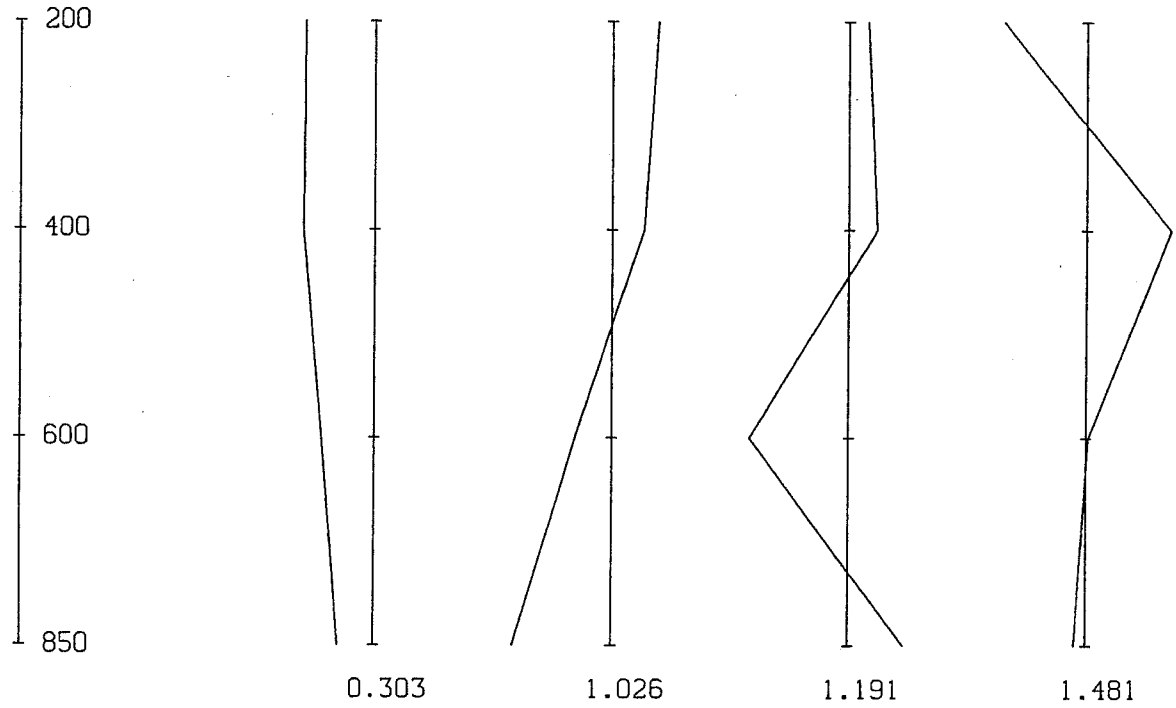


Fig. 8 Eigenvalue and vector decomposition of the narrow prediction error correlation matrix for 4 thickness layers centred at the pressure values shown to the left. The 4 eigenvector are plotted against a vertical axis with value 0. The number below the axes are the corresponding eigenvalues.

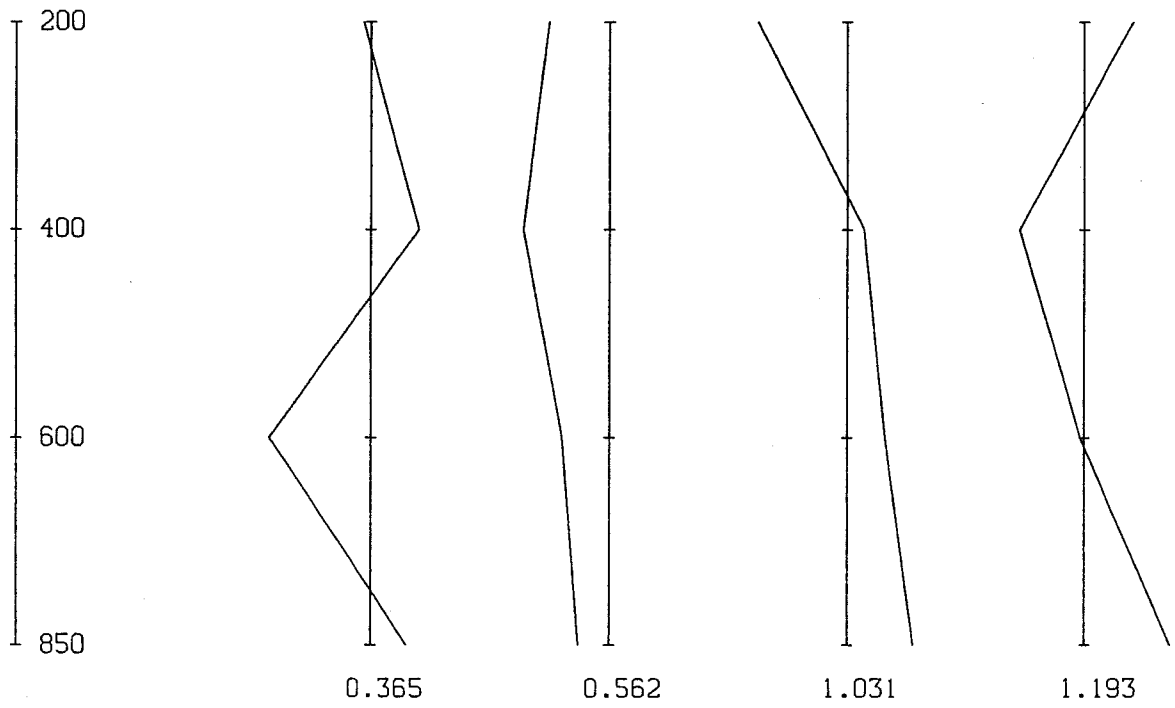


Fig. 9 Same as Fig. 8, but for the (normalized) observation error correlation matrix for clear satellite soundings.

eigenvalue, i.e. the most accurately predicted mode, is the mean temperature. The second most accurate mode is the predicted gross static stability. The two least accurately predicted modes are higher internal modes with less well defined error structures. This ordering of the accuracy of the forecast error modes is quite reasonable.

The normalized observation error covariance matrix has been decomposed in a similar way. Fig. 9 shows the eigenvalues and vectors for a clear satellite sounding. According to the specified observation error covariances the most accurately observed mode is the thin layer static stability. The second most accurate mode is the tropospheric mean temperature. From the filtering point of view the response to data is proportional to the ratio of the eigenvalue of a particular forecast error mode to the sum of the eigenvalues of the same forecast and observation modes. The weight matrix reflects the response to the 4 modes in terms of the eigenvalues (Fig. 10). The smallest eigenvalue (ratio of output to input) is found for the mean tropospheric temperature and the highest eigenvalue (best analysis response) for thin layer stability. This response is contradictory to our knowledge of the usefulness of the various modes of the satellite observations. This explains why the ECMWF analysis scheme draws very poorly to the mean tropospheric satellite temperature. The OI scheme responds very strongly to profiles in which adjacent departures have different signs.

(ii) Modified observation error covariance matrix

As the prediction error covariance matrix appears to be reasonable, it is only possible to modify the analysis response by modifying the observation error covariance matrix. As the satellites are best in observing deep layer mean temperatures, an $\underline{\underline{O}}$ matrix having an accurate tropospheric mean temperature and much less accurate higher modes, has been constructed and tested (Fig. 11). The eigenvalues and vectors of the weight matrix using the modified $\underline{\underline{O}}$ matrix are shown in Fig. 12. The structures of the eigenvectors of the $\underline{\underline{W}}$ matrix are not as clear as for the P matrix. However, the best response is to a mode which is best described as the mean temperature between surface and 300 hPa. The weakest response is to the gross tropospheric stability. This modified version of the scheme draws very closely to the lower tropospheric thicknesses.

3.2 Interpolation to model levels

A necessary requirement for an analysis response that reflects the assumed error characteristics is an $\underline{\underline{O}}$ matrix with small errors in the deep layer mean temperature. This then gives a reasonable analysis of the observed quantities at the observation positions. The second problem is to interpolate the filtered analysis at the observation points to the model levels and calculate temperature changes in the model coordinates (horizontal and vertical). Only the vertical problem will be considered in this paper.

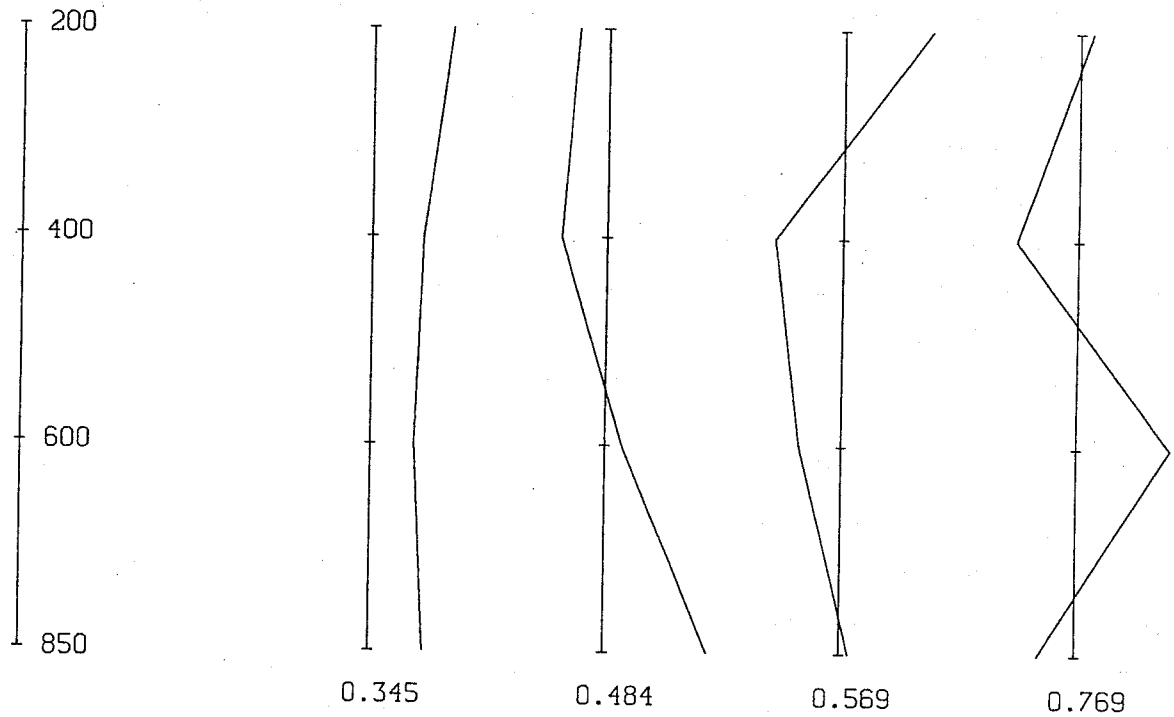


Fig. 10 Same as Fig. 8, but for the weight matrix in an analysis using one clear satellite sounding with narrow vertical prediction error correlation matrix.

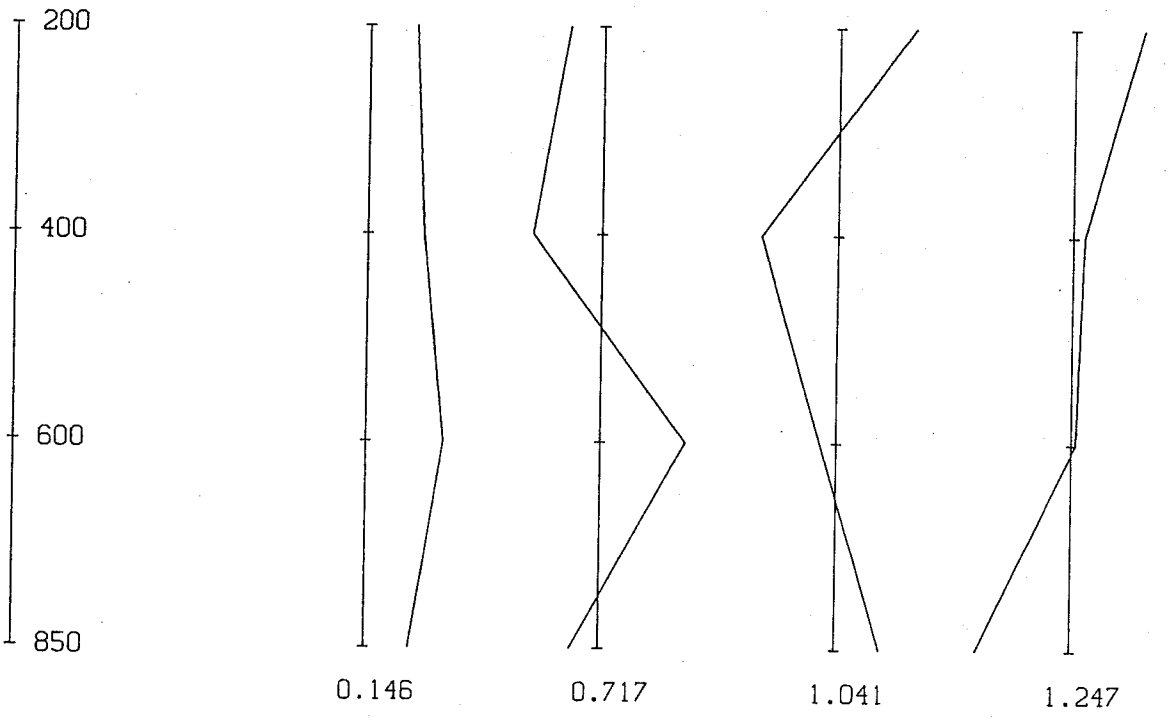


Fig. 11 Same as Fig. 8, but for a modified (normalised) observation error correlation matrix.

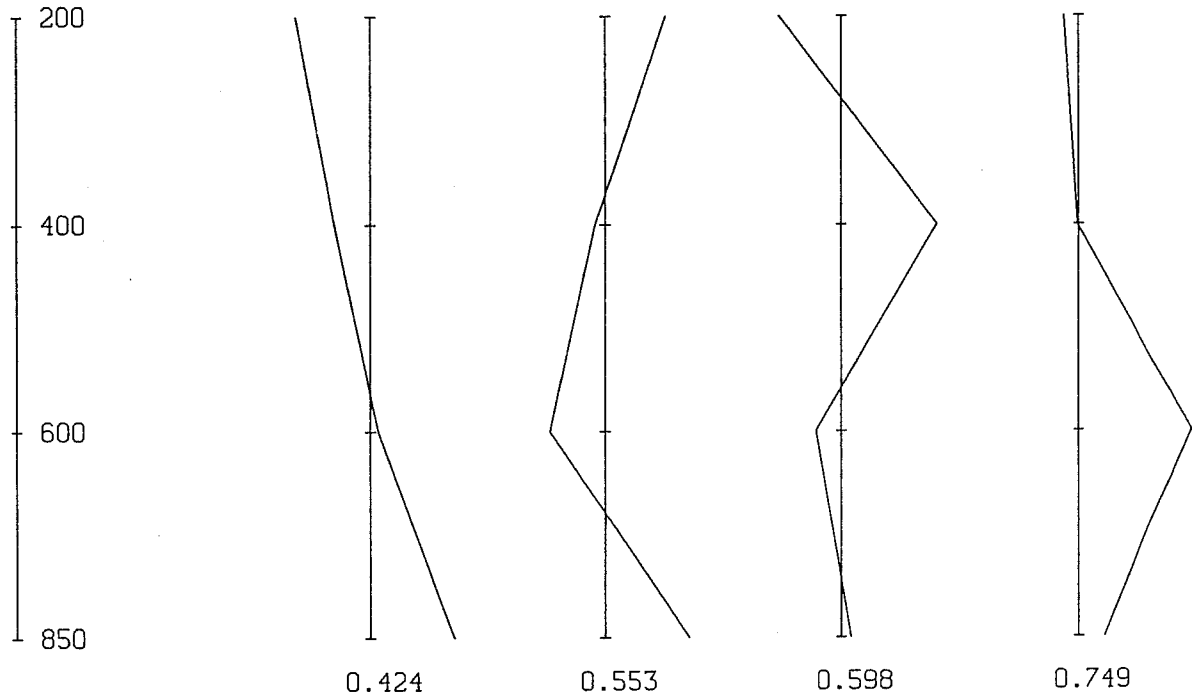


Fig. 12 Same as Fig. 10, but using the modified observation error correlation matrix shown in Fig. 11.

(i) Operational scheme

The response at model levels for the operational scheme is shown in Fig. 13. The observed input was a constant 1 K departure given as 7 thicknesses. The output profile, shown in Fig. 13, has large variations in particular in the boundary layer where the prediction error correlations are quite sharp. Near 750 hPa there are no temperature increments. The strongest response in the boundary layer is about 1/3 of the input.

(ii) Operational case using wide $\underline{\underline{P}}$ covariances

The vertical forecast error covariances are assumed to have a wider vertical structure over the eastern Pacific than elsewhere (Lönnberg, 1989). The response at model levels using the wide $\underline{\underline{P}}$ covariance matrix is shown in Fig. 14. The profile of the temperature increments is much smoother than the one using narrow prediction error covariances (Fig. 13). Although the profile is smooth the response is still very weak to a constant input of 1K.

(iii) Modified input

It has been shown that the lower tropospheric layer 700-1000 hPa has a large systematic and random error (Andersson et al., 1989 and Strauss, 1989). As this layer contributes little and may actually have a detrimental impact, it might be better to use a satellite profile from 700 to 100 hPa instead. Fig. 15 shows the analysis response in the operational case of constant input using wide $\underline{\underline{P}}$ covariances. The only difference between Fig. 15 and 14 is the omission of the 700/1000 hPa input datum. The response is reasonable for the layers of data (700-100 hPa), but outside the data layer a compensation occurs in the lowest layer such that the height increment goes towards zero near the surface. This causes a temperature increment which is opposite to that in the layer above thereby changing the stability at the bottom of the data layer significantly. It is clear that in order to control the output, the input has to specified as a complete profile.

(iv) Use of thick layers

Several experiments of combining layers have been done. The results from one of them will be described in the following. In this response experiment the layers 1000-700 and 700-500 hPa have been combined. The response within the thick layer is difficult to control (Fig. 16). The increment even changes sign within that, producing wild oscillations for the whole temperature profile. This case is not strictly comparable to the earlier cases (i)-(iii), as the input profile has been specified as constant normalized departures.

3.3 Discussion

The calculation of increments in the model coordinates can be regarded as a two-step process: filtering of noise in the data, i.e. analysis at the observation points, and

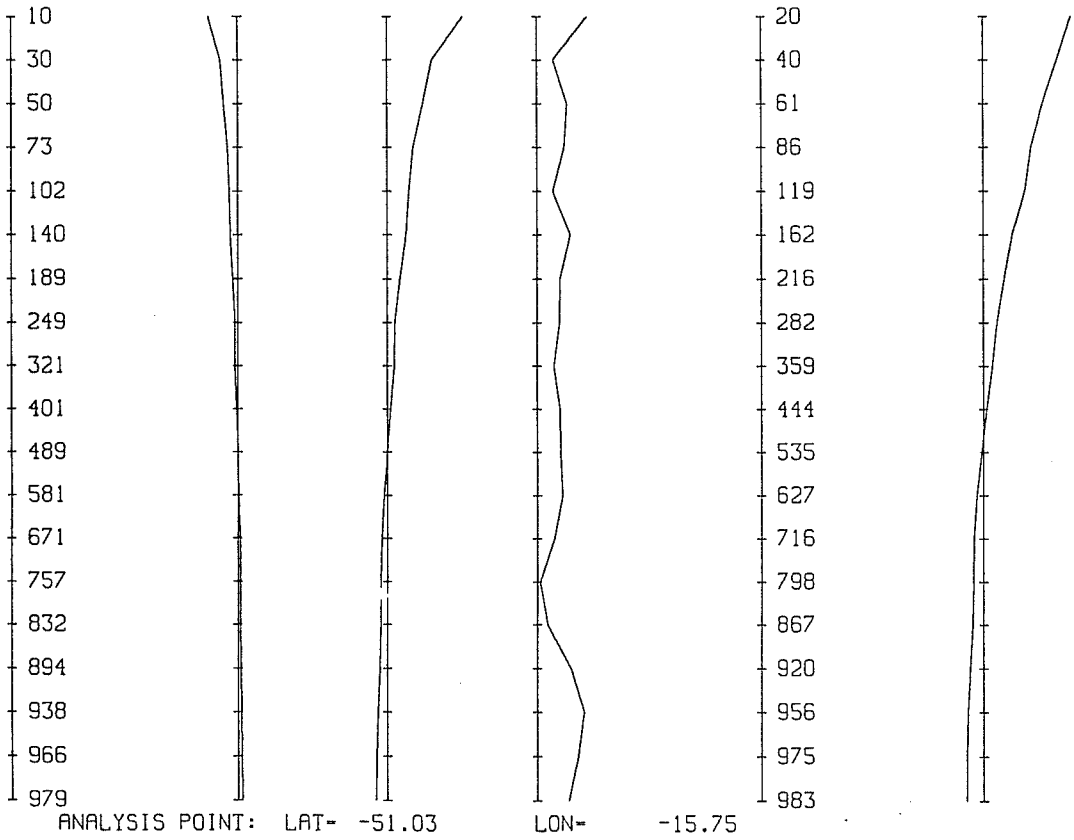


Fig. 13 Analysis increments at model levels for u, v and T (left part) and 2 (right part) using one clear satellite sounding with a 1K departure from background at all 7 layers. Narrow vertical prediction error correlations have been used.

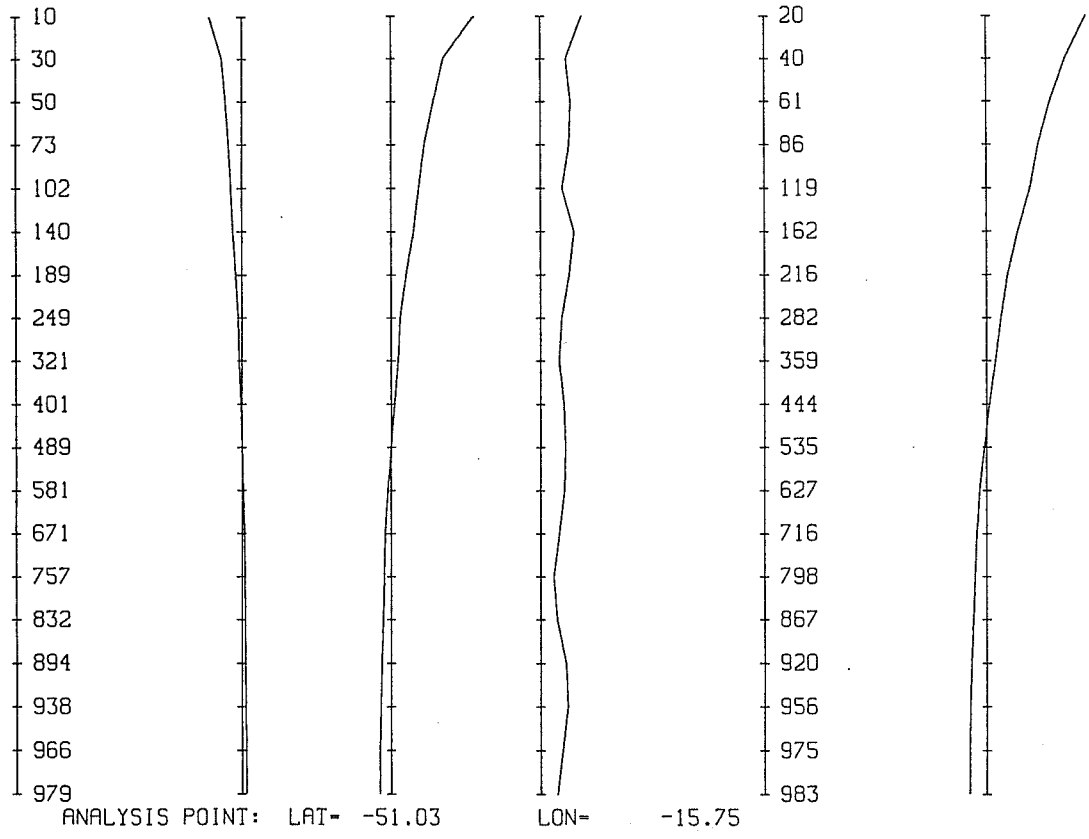


Fig. 14 Same as Fig. 13, but using wide vertical prediction error correlations.

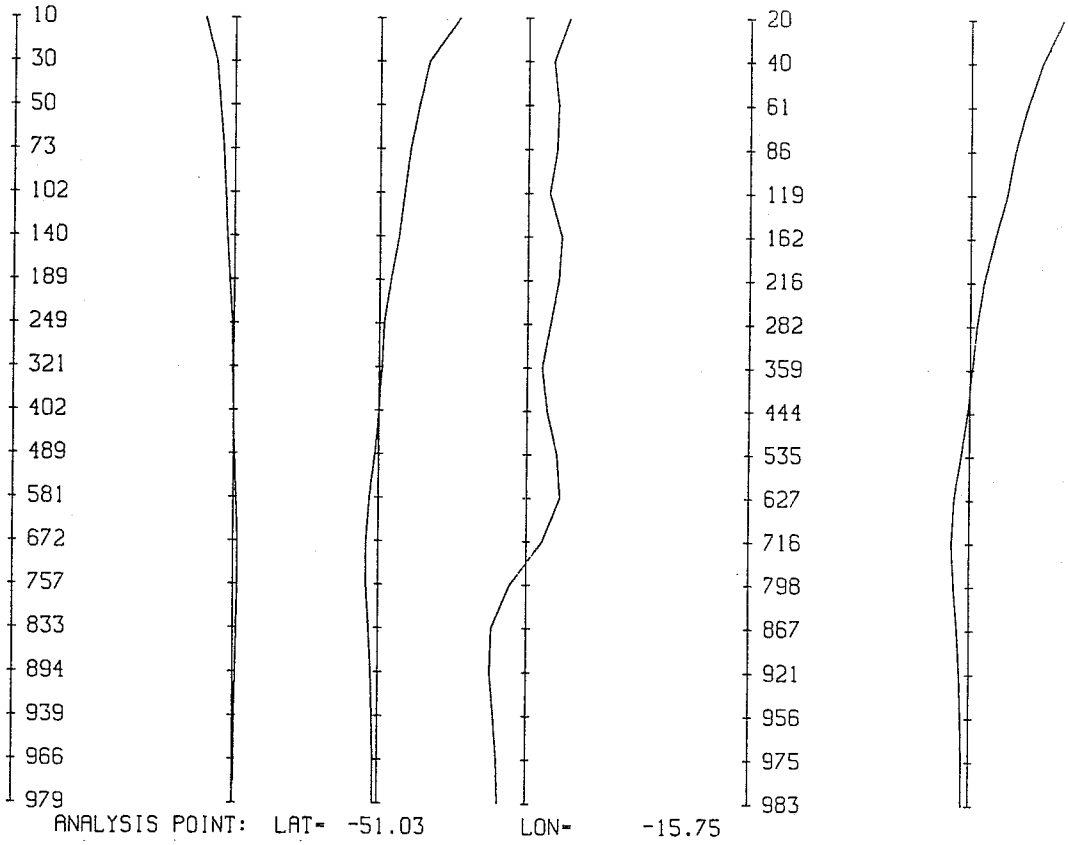


Fig. 15 Same as Fig. 14, but for an incomplete sounding (700-10 hPa).

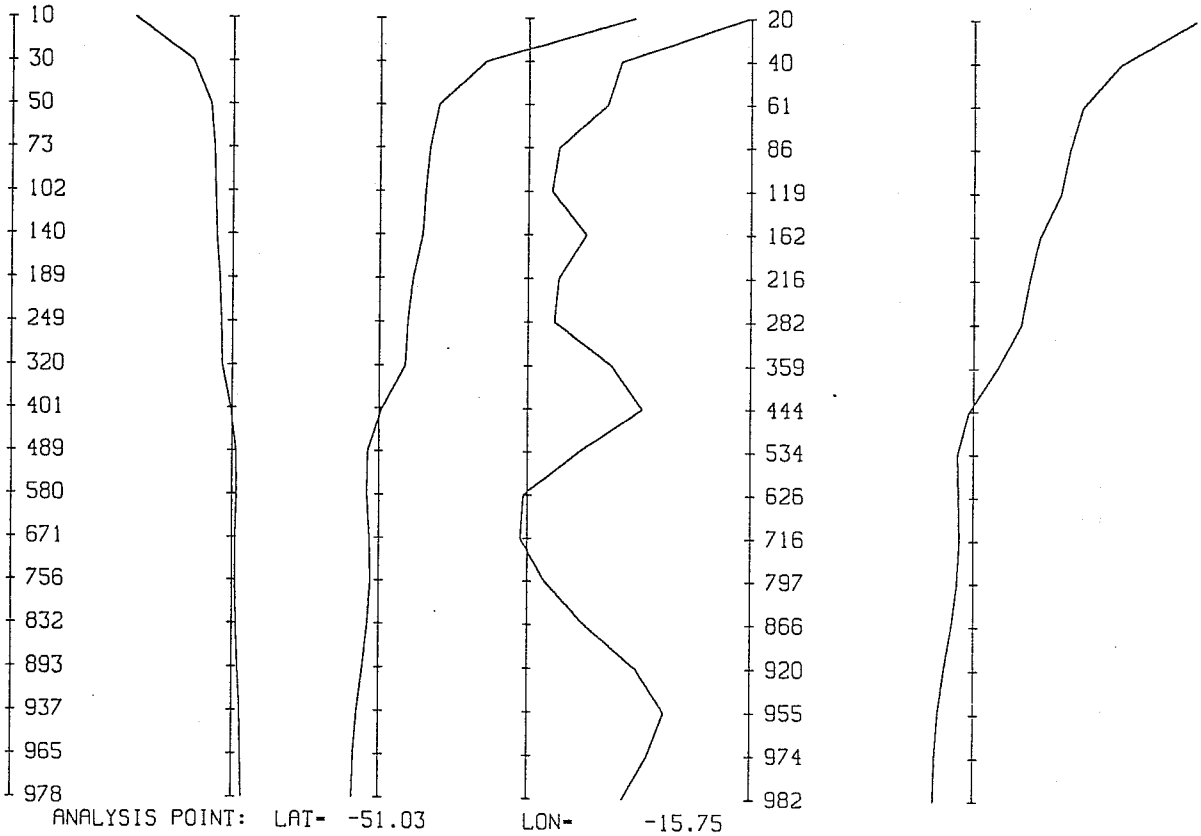


Fig. 16 Same as Fig. 13, but the data layers 1000-700 hPa and 700-500 hPa have been combined to one datum (1000-500 hPa). The input are constant normalized departures.

interpolation of the filtered analysis from the data points to model coordinates (Hollingsworth, 1987). Both processes are complicated for satellite data as the OI variable is height and the input data are thicknesses and the analysis output is temperature. Careful tuning of the P and O matrices is necessary to obtain proper filtering properties at the data points. However, to control the output on model levels it is necessary to have a sufficient number of data points.

## 4. CONCLUSIONS

Remotely sensed observations provide a good data coverage over most the globe. However, these observing systems do not directly observe the quantities used by numerical models. In the transformation to quantities which are readily used by data assimilation schemes, systematic errors and inherent difficulties in these transformations degrade the data. The data user regards these as serious random and systematic errors and protects the analysis by complicated QC algorithms. As the remotely sensed data is potentially most useful in data sparse regions, serious efforts on QC are required. The only reliable information in these regions is the background field. It then becomes crucial to know the error characteristics of the short range forecast and in particular it becomes vital to know whether a large departure is caused by a poor forecast or by a corrupt observation. The statistical knowledge of the distribution of the departures, in particular the extreme parts of the distribution, is essential to establish from high quality observations. By comparing the distributions of reliable data with those for satellite observations it is possible to estimate likelihood of gross satellite observation errors. Ideally, a dynamic QC should be implemented using reliable stations as guides.

The other complication with satellite data are their error structures. This requires careful tuning of the error covariances used in the OI scheme to extract the accurately observed modes and filter out the less reliable modes. Although the information content of a satellite sounding is only a few items, it is necessary to provide the observation input in several layers in order to minimise the interpolation error in going from thick layer data to thin layer temperature changes at model levels.

## References

Andersson, E., J.F. Flobert, G. Kelly, J. Pailleux and Z. Zhang, 1989: Impact of satellite sounding data in the ECMWF system. In this volume.

Hollingsworth, A., 1987: Objective Analysis for Numerical Weather Prediction. In: Short and Medium Range Numerical Weather Prediction. Collected papers presented at WMO/IUGG NWP Symposium, Tokyo, 4-8 August, 1986, ed. by T. Matsuno, Special Volume of the J.Meteor.Soc.Japan. 11-59.

Hollingsworth, A. and P. Lonnberg, 1986: The statistical structure of short range forecast errors as determined from radiosonde data. Part I: The wind field. Tellus, 38A, 111-136.

Kelly, G., E. Andersson, P. Lönnberg, J. Pailleux and Z. Zhang, 1989: Quality control of TOVs data on the ECMWF analysis and forecast systems. In this volume.

Kelly, G. and J. Pailleux, 1989: A study assessing the effects of new methods producing cloud track winds using the ECMWF analysis and forecast systems. In this volume.

Kelly, G.A. and J. Pailleux, 1988: Use of satellite vertical sounder data in the ECMWF analysis system. ECMWF Tech.Memo., No.143, 46 pp.

Lönnberg, P., 1988: Developments in the ECMWF analysis system. Proceedings of the ECMWF seminar on data assimilation and the use of satellite data, Reading 5-9 September 1988.

Radford, A., 1989: Monitoring of cloud-motion winds at ECMWF. In this volume.

Schmetz, J. and M. Nuret, 1989: Cloud motion wind estimates in Europe. In this volume.

Strauss, B., 1989: Monitoring of TOVS/DMSP data. In this volume.